Superalloys 2012: 12th International Symposium on Superalloys
Edited by: Eric S. Huron, Roger C. Reed, Mark C. Hardy, Michael J. Mills, Rick E. Montero, Pedro D. Portella, Jack Telesman
TMS (The Minerals, Metals & Materials Society), 2012

High Temperature Creep of New $L1_2$-containing Cobalt-base Superalloys

Michael S. Titus[1], Akane Suzuki[2], Tresa M. Pollock[1]

[1]Materials Department, University of California Santa Barbara; Santa Barbara, CA, 93106-5050, USA
[2]GE Global Research, One Research Cr.; Niskayuna, NY, 12309, USA

Keywords: Cobalt alloys, High temperature creep, Single-crystal, Directional coarsening

Abstract

High temperature deformation in single crystal Co-Al-W-base γ-γ' alloys containing Ti, Ta, and Cr has been investigated. The alloys contain a initial two phase microstructure consisting of ordered ($L1_2$) precipitates embedded in a solid-solution FCC matrix, similar to Ni-base alloys. Tension creep tests of single crystal Co-base alloys have been conducted in vacuum at 900°C at stresses between 275 and 379 MPa. Minimum creep rates of these Co-Al-W-base alloys are comparable to commercial Ni-base superalloy René N4. Directional coarsening and the formation of W-rich phases are observed during creep. Implications for future design of the Co-base alloys are discussed.

Introduction

Nickel-base superalloys have seen decades of use in gas turbine applications due to their superior creep resistance at high temperatures [1, 2, 3]. Successive generations of improved alloys have substantially improved turbine performance. For example, turbine inlet temperatures in industrial gas turbines have increased due to the introduction of advanced nickel-based single crystals, resulting in a combined cycle power plant efficiency near 60% [4]. It is estimated that a 1% increase in efficiency saves $15-20M over the lifetime of a land-based gas turbine engine [4]. Thus, there is a continued incentive to develop higher temperature materials. Current Ni-base alloys are reaching their operational temperature limit due to the onset of melting in these alloys, which is typically in the range of 1350-1450°C [1, 5].

Numerous strategies have been developed to increase the operating temperature of gas turbine engines. In the 1960s, the first designs with internal cooling passages that draw air from the compressor were introduced [5, 6]. The development of serpentine cooling passages and film cooling, provided by laser drilled cooling holes on the pressure side of the blade, again allowed for operating temperatures to increase [3]. These cooling methods further challenge the thermomechanical performance of the superalloy in service [7]. The newest technology involves the use of bond coats and thermal barrier coatings that protect the underlying cooled superalloy from extreme temperatures [5, 6]. Due to the potential for foreign object damage, the ability of thermal barrier coatings to increase engine operating temperature will ultimately be limited by the maximum operating temperature of the superalloy substrate [6]. As an alternative to developing these new and complex technologies, increasing the temperature capability of the metal substrate could increase the operating temperature of the engine.

Recently, the existence of an $L1_2$ phase in the Co-Al-W ternary was discovered [8]. Alloys containing a two-phase (γ-γ') microstructure, similar to Ni-base alloys, have subsequently been subjected to preliminary investigations. The γ crystal structure is face-centered cubic (A1), and the Co_3(Al,W) γ' precipitates are of $L1_2$ structure [8]. The Co-base alloys have liquidus temperatures of about 100-150°C higher than CMSX-4 containing 3wt.% Re suggesting a potential temperature benefit equivalent to several generations of new alloys [9, 10].

These new cobalt-base alloys are resistant to freckle formation during directional solidification, which is beneficial for casting of physically large components [11]. Compressive flow stress experiments have also shown that Co-Al-W-Ta single crystals exhibit a larger 0.2% flow stress than Ni-base superalloys above 900°C [12]. These initial studies provide further motivation to study high temperature creep, which is a dominant mode of deformation for single crystal turbine blades used in gas turbine engines [13].

Experimental Methods

Four alloys have been investigated and their compositions are given in Table 1. Alloying additions of

Table 1: Compositions in at.% of Co-base alloys investigated.

Alloy	Co	Al	W	Ta	Cr	Ti
Ternary	79.9	9.4	10.7	-	-	-
2Ta	79.4	8.8	9.8	2	-	-
CrTa	78.4	7.8	7.8	1.5	4.5	-
6Ti	79	6.7	8.1	-	-	6.2

Cr, Ta, and Ti were investigated for their influence on the γ'-solvus temperature, oxidation resistance and creep resistance.

Single crystal bars of [001] orientation about 152 mm in length and 20 mm in diameter were cast *via* the conventional Bridgman technique. A withdrawal rate of 200 mm/hr was used. All alloys were subsequently solution heat treated then aged in a vacuum resistance furnace backfilled with argon according to the schedules given in Table 2.

Ends of the heat treated bars were sectioned and metallographically prepared to examine the γ-γ' microstructure. An etchant comprised of 20 mL HCl - 10 mL H_2O_2 was used to reveal both the dendrites and γ-γ' microstructure. The etchant preferentially attacks the γ phase.

The primary dendrite arm spacing (PDAS), area fraction of porosity and γ' area fraction were measured for each alloy. Five light optical images of the solution heat treated specimens in the etched condition were used to determine PDAS using conventional methods [14]. Five light optical images of aged specimens in the as-polished condition were used to determine the average area fraction porosity using ImageJ. A one-way analysis of variance (ANOVA) was conducted between each of the four compositions to determine statistical differences of the measured porosity between the four compositions. Five backscatter electron images using a FEI XL-30 scanning electron microscope (SEM) were used to measure the area fraction on high constrast images of the γ' precipitates using ImageJ.

Table 2: Heat treatment schedules of investigated alloys.

Alloy	Solution	Age
Ternary	1350°C/12hrs	950°C/120hrs
2Ta	1350°C/12hrs	1000°C/100hrs
CrTa	1300°C/6hrs	900°C/150hrs
6Ti	1225°C/60hrs	1000°C/100hrs

Table 3: Constant load tensile creep test conditions.

Sample	Temp. (°C)	Stress (MPa)	End of Test
Ternary	900	310	Rupture
		345	Int. at 2%
2Ta	900	310	Rupture
		345	Int. at 2%
CrTa	900	310	Int. at 2%
		275	Rupture
6Ti	900	310	Int. at 2%
		379	Rupture

Differential thermal analysis (DTA) was performed on the investigated alloys using a Seteram Setsys 18 system with a Pt reference sample. The system was calibrated with high-purity Ni and Ag prior to experiment [15]. Solution heat treated cylindrical specimens with a mass ranging from 250 to 350 mg were prepared, and transformation temperatures were determined using cooling curves for γ'-solvus, and heating curves for the solidus and liquidus, at a rate of 5 K min^{-1}.

Button head tensile creep specimens 76.2 mm in total length with a 25.4 mm gage length were machined from the single crystal bars. Vacuum creep studies were conducted in tension at 900°C at stresses between 275 - 379 MPa using a 3:1 lever arm. An overview of creep testing conditions is given in Table 3. All tests were conducted at a vacuum level below 10^{-6} torr. The temperature on the sample was measured using a bare-tip R-type thermocouple which was in contact with the gage section prior to the onset of the creep test. Strain was measured by taking the average of two linear voltage capacitor transducers which measured displacement of the extensometer attached to grooves at either end of the gage section.

Microstructure and Physical Properties

The PDAS in the as-solidified bars were 247, 139, 175 [11], and 315 μm for the Ternary, 2Ta, CrTa,

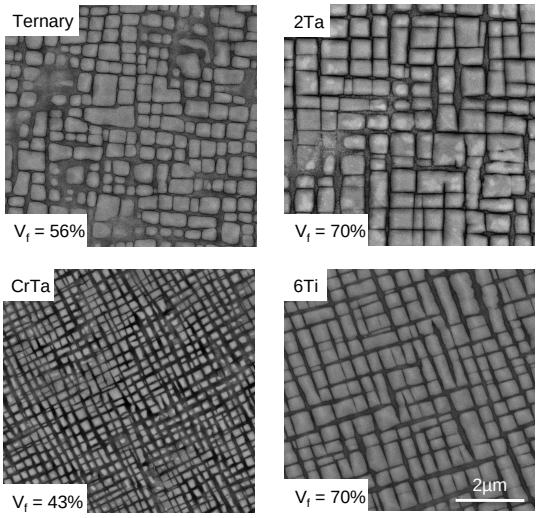

Figure 1: Backscatter SEM images of γ-γ' microstructure in the aged and etched condition. The γ' phase is lighter in the images.

and 6Ti alloys, respectively. The as-cast microstructure contained eutectic pools in the interdendritic regions, and precipitates which varied in size and morphology. Larger precipitates about $0.4\,\mu m$ in diameter were found in the interdendritic regions, while smaller precipitates ($<0.1\,\mu m$) were found in the dendrite cores.

Solution heat treated samples of 2Ta and 6Ti did not contain any remnant eutectic phases, while the Ternary and CrTa showed a very limited amount of eutectic phases. The porosity area fraction for the fully heat treated Ternary, 2Ta and CrTa alloys was less 0.5%. The 6Ti alloy exhbited area fraction porosity at about 1%. The one-way analysis of variance results verified the difference in mean area fraction of porosity between the 6Ti and other three alloys.

The morphology of the γ' precipitates in all the aged Co-base alloys was cuboidal, as shown in Figure 1. The size of the cubes was about 0.4 - $0.6\,\mu m$ for the Ternary, 2Ta, and 6Ti alloys, and less than $0.2\,\mu m$ in the CrTa alloy. The γ' volume fraction varied from about 40% - 70%, as shown in Figure 1.

The transformation temperatures as measured by DTA are given in Figure 2. Data from reference [16] shows γ'-solvus, solidus and liquidus of 1309°C, 1326°C, and 1370°C, respectively for CMSX-4.

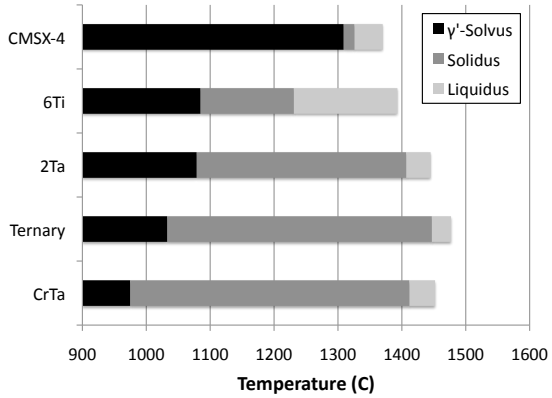

Figure 2: Liquidus, solidus [11] and γ'-solvus temperatures of the investigated alloys, compared to CMSX-4 [16].

Single Crystal Tensile Creep

Figure 3 shows selected creep curves of the four alloys at several different stresses. Limited primary creep (<0.3%) was observed in all tested alloys. Due to limited primary creep, the minimum creep rate was established within the first hour in all tests, and this rate persisted for 20-100 hrs, depending on the alloy and testing conditions. The minimum creep rate as a function stress for all tested specimens is shown in Figure 4.

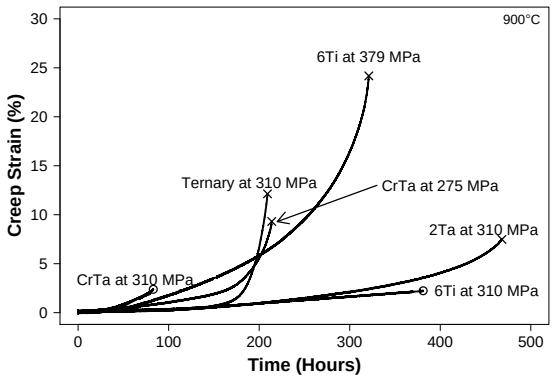

Figure 3: Creep curves of selected tension creep tests conducted at 900°C. Open symbols (○) at the end of a curve represents an interrupted test, and an "X" represents a test conducted to rupture.

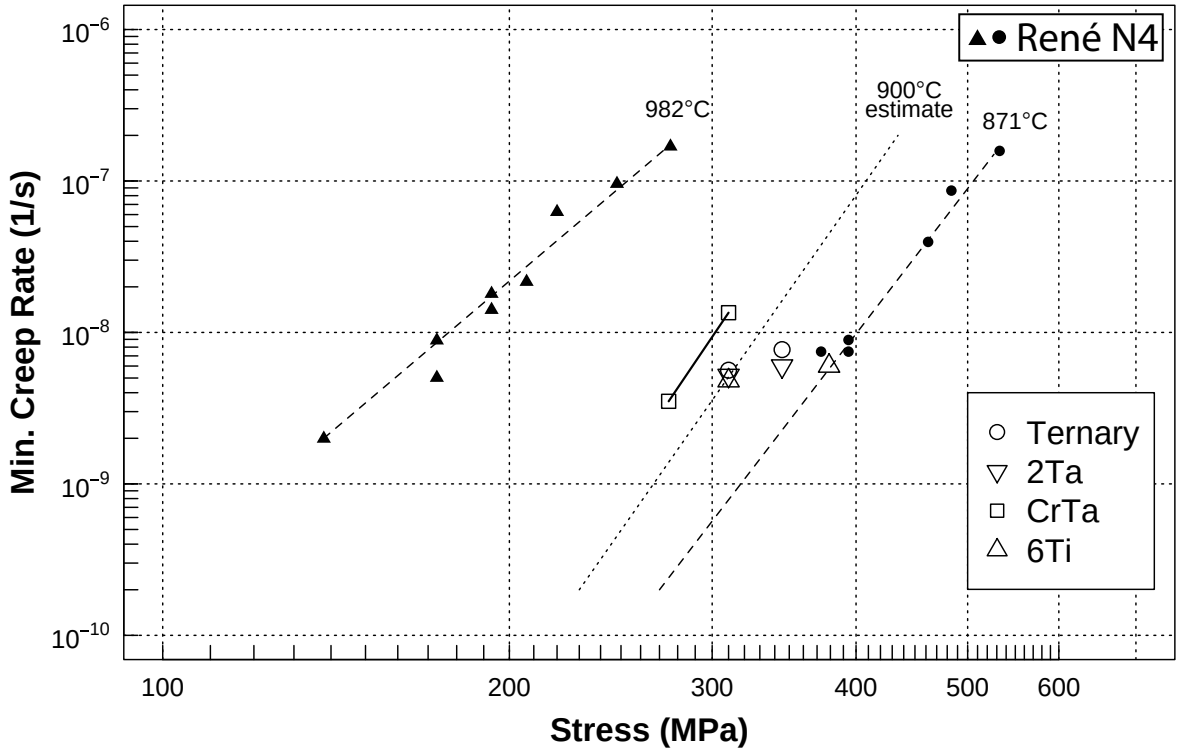

Figure 4: Minimum creep rate (s^{-1}) as a function of stress (MPa) of tested Co-base creep specimens at 900°C. The filled data points are data from commercial alloy René N4 [17]. A 900°C estimate has been interpolated from the René N4 data.

Directional coarsening (rafting) of the γ' precipitates occurred parallel to the applied tensile axis in all rupture specimens, as shown in Figure 5. Coarsening parallel to the applied tensile stress is indicative of positive misfit between the γ and γ' phases [18]. The sign of misfit is in agreement with previous x-ray diffraction studies [8].

The rafts varied in thickness, according to the initial precipitate size. The CrTa alloy contained the smallest initial precipitates and developed significantly thinner rafts compared to the Ternary, 2Ta, and 6Ti alloys. The 6Ti alloy contained the most irregular rafts of the alloys investigated.

Undesired phases not present in the as-aged material precipitated during creep in the 2Ta and CrTa alloys, as shown in Figure 6. The morphology of the plate-like phases is similar to the Co_3W ($D0_{19}$) phase which has been characterized in diffusion couple and oxidation experiments [9, 19].

Shear bands developed during creep at high strains in the Ternary, 2Ta, and CrTa alloys (see arrows in Figure 6). The bands were oriented at approximately 45° to the loading axis. Along the shear bands, W-rich phases precipitated in the 2Ta and CrTa alloys. There was no preference for the formation of the W-rich phases in the interdendritic regions.

Longitudinal cross sections revealed that W-rich phases were concentrated along the exterior, exposed surface in the gage section of the 2Ta and CrTa specimens, but decreased in apparent area fraction towards the center. This may be due to local Al depletion from limited vaporization in the vacuum chamber. No oxide scale was observed on the surface. The W-rich phases did not appear to be concentrated on the fracture surface of the specimens, though the fracture surface was sloped along the same direction as the shear bands.

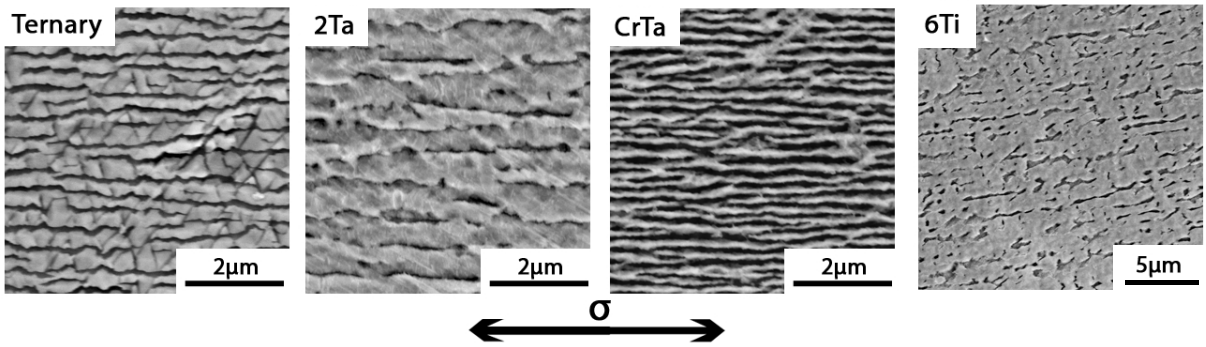

Figure 5: Backscatter SEM images of etched specimens crept to rupture. The γ' phase is lighter in the micrographs.

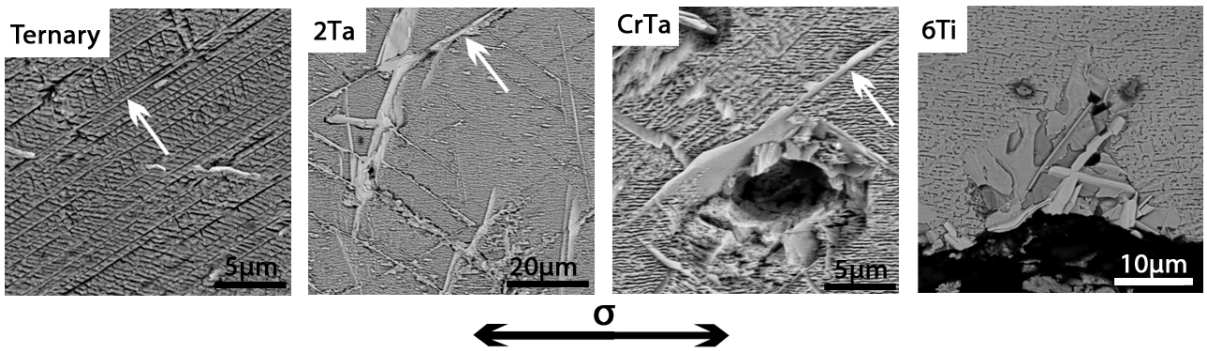

Figure 6: Backscatter SEM images of etched specimens crept to rupture. Tungsten-rich phases are formed during creep and tend to form along the shear bands (arrows).

The ruptured 6Ti specimen also contained W-rich phases near the outside, exposed surface in the gage section where some recrystallization occurred, as shown in Figure 6. No W-rich phases were observed subsurface, or along the fracture surface.

In all alloys, the tertiary regime of creep accounted for greater than 50% of the rupture life for all specimens, and all specimens tested to rupture failed with less than 24% creep strain. Figure 7 shows a Larson Miller curve the Co-base alloys in comparison to a number of commercial single crystal alloys. The 6Ti alloy exhibited the longest rupture life, and the CrTa alloy exhibited the lowest rupture life in the alloys investigated.

In the Ternary, 2Ta, and CrTa specimens, the fracture surface appeared relatively smooth and was sloped approximately 45° from the tensile axis. The fracture surface of the 6Ti specimen was significantly rougher than the other three alloys, and was oriented approximately normal to the axis of the applied stress. The cross-sectional areas of the gage length experienced shape changes after extensive deformation in the Ternary, CrTa, and 6Ti specimens. The gage sections of the Ternary and 6Ti alloys experienced a change in cross section, elongating along the transverse [100] direction. Conversely the CrTa alloy elongated along the [110] direction, as shown in Figure 8. The 2Ta ruptured specimen maintained a cylindrical shaped gage section. An overall summary of these creep properties is given in Table 4.

Discussion

Initial microstructures of the Co-base alloys show a strong dependence on chemistry and heat treatment, with varying γ' precipitate volume fraction and size. The Ternary, 2Ta, and 6Ti alloys all possess a high volume fraction and relatively large size of precipitates as a result of aging above 950°C, whereas the CrTa alloy exhibits a lower volume fraction

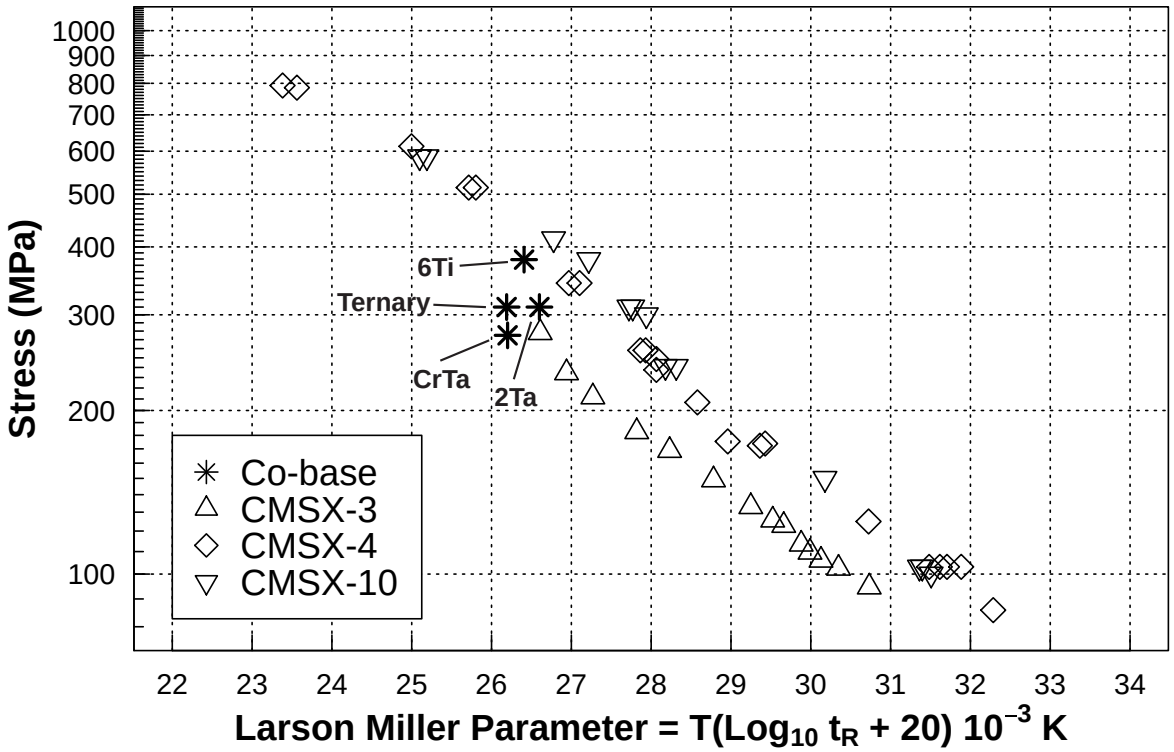

Figure 7: Stress vs. Larson Miller Parameter (where T is temperature (K) and t_R is rupture life (hours)) for investigated alloys compared to 1st, 2nd, and 3rd-generation superalloys CMSX-3, -4, and -10 from Refs. [20, 21, 22, 23, 24].

and smaller size of precipitates after a 900°C heat treatment. Tantulum and Ti are γ'-forming elements while Cr is a γ-forming element in Co-base alloys [8, 25]. The CrTa alloy has the lowest γ'-solvus temperature among the set of alloys investigated, at 975°C. In Ni-base alloys, the volume fraction of γ' typically decreases with increasing temperature [26, 27]. Apparently, the lowering of the γ'-solvus is caused by Cr additions with the net effect of producing low volume fractions of precipitates in spite of a lower aging temperature.

The DTA experiments shown here, and experiments conducted by Ooshima *et al.* [25] indicate that the γ'-solvus temperature increases monotonically with W content in the Co-Al-W alloys. Additions of 6Ti and 2Ta increase the γ'-solvus temperature by about 50°C compared to the ternary alloy. The γ'-solvus temperature of the 2Ta alloy is 9°C greater than the alloy studied by Ooshima *et al.* which had 2at.% less W content. Additions of Ti up to 6at.% appear to be beneficial to the γ'-solvus temperature as it increases the transformation by about 60°C compared a similar Co-Al-W-2at.%Ti alloy investigated by Ooshima *et al.* However, Ti widens the freezing range and lowers the solidus temperature. Chromium additions have been shown to decrease the γ'-solvus temperature in Co-Ni-Al-W-base alloys [28], and Co-base studied here and by Ooshima.

Comparison of the minimum creep rates (Figure 4) for the Co-base alloys and commercial superalloy René N4 suggest that the Co-base alloys are performing comparably or better at 900°C. This is remarkable considering the Ternary alloy is simple with regard to chemistry. A prior polycrystalline creep test of a Co-Al-W-0.1at.%B alloy at 850°C and 350 MPa exhibited a minimum creep rate of about $4 \times 10^{-8}\,\mathrm{s}^{-1}$ [29]. In the present study, the Ternary alloy tested at 900°C and 345 MPa resulted in minimum creep rate of $8 \times 10^{-9}\,\mathrm{s}^{-1}$. Thus the single crystal alloys show a temperature benefit in

Table 4: Overview of creep properties of investigated alloys.

Sample	Temp. (°C)	Stress (MPa)	Min. Creep Rate ($10^{-8}s^{-1}$)	Time to 2% (hrs)	Final Creep Strain (%)	Time to Rupture (hrs)	Rafting Direction	Initial Precipitate Shape
Ternary	900	310	0.6	175	12(rup)	209	Parallel	Cuboidal
		345	0.8	80	2.1(int)	-		Cuboidal
2Ta	900	310	0.5	295	7.4(rup)	468	Parallel	Cuboidal
		345	0.7	190	1.98(int)	-		Cuboidal
CrTa	900	310	1.4	65	2.2(int)	-		Cuboidal
		275	0.4	133	9.7(rup)	214	Parallel	Cuboidal
6Ti	900	310	0.5	356	2.3(int)	-		Cuboidal
		379	0.6	107	24.1(rup)	321	Parallel	Cuboidal

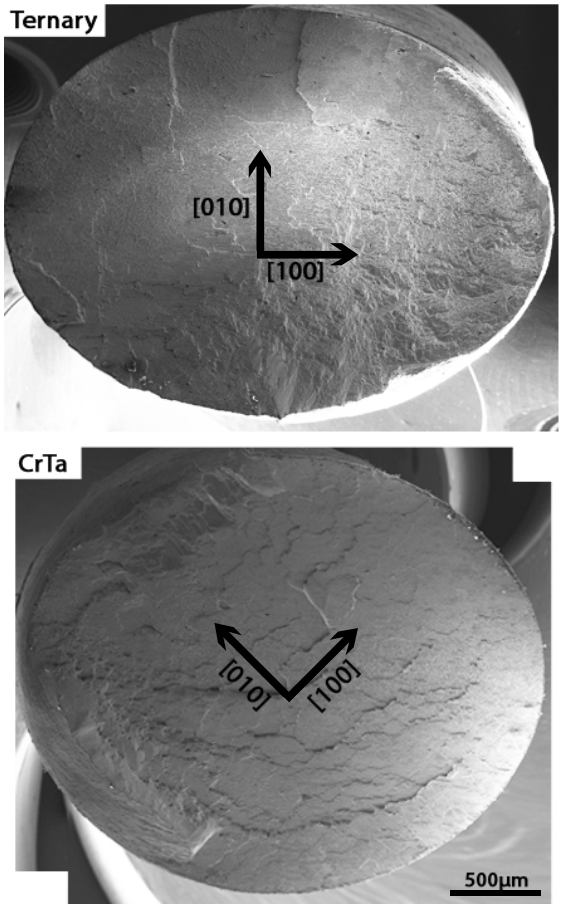

Figure 8: Cross section shape changes in the Ternary and CrTa alloys tested at 345 MPa. Images were stitched and blended together.

creep properties by at least 50°C.

The minimum creep rates of the 2Ta and 6Ti alloys are lower than those exhibited by new Ni-containing Co-Al-W alloys with additions of Ta, Cr, Mo, B and C [28]. The time to accumulate 2% creep strain is also longer in the Co-base alloys relative to the Co-Ni-Al-W-base alloys. The reasons for this are not yet clear; further systemic studies with controlled Ni additions would be useful.

The Co-base rafts are longer and of higher aspect ratio than the Co-Ni-Al-W-base rafts that formed during creep. Work by Caron *et al.* [30] showed that, for specimens with an initial well-aligned array of cuboidal precipitates, the minimum creep rate was lower than specimens containing initially irregularly shaped particles. The authors concluded that the well-aligned cuboidal precipitates facilitated a rapid formation of high aspect-ratio rafts. Mughrabi suggested that if dislocations cannot cut the γ' rafts, elongated rafts would be beneficial to creep properties because the rafts would prohibit dislocations from climbing and gliding around them [31]. Comparison of the microstructures reveals that the Co-base alloys have a more regular array of γ' precipitates than the Co-Ni-Al-W-base alloys [28], which is likely responsible for improved creep properties.

Figure 7 compares the Larson Miller Parameter (here given in Kelvin) of the investigated Co-base alloys to 1st-, 2nd-, and 3rd-generation Ni-base superalloys CMSX-2, -3, and -10, respectively. All Co-base alloys investigated are comparable or superior to CMSX-3, with regards to rupture life. The 6Ti alloy exhibits a rupture life comparable to CMSX-4 - a 2nd-generation superalloy.

First-principles density functional theory calculations using special quasi-random structures has indicated that Ti additions to the γ'-Co_3(Al,W) phase increase the superlattice intrinsic stacking fault energy [32]. An increase in stacking fault energy would provide a greater energy barrier to dislocation penetration in the γ' phase. The increase in stacking fault energy may help explain why the 6Ti alloy exhibited the lowest minimum creep rate and largest rupture creep strain of all alloys investigated. Additionally, phase diagrams of the Co-Al-W-Ti quaternary developed by Kobayashi *et al.* [33] indicated that there exists a stable $L1_2$ field spanning from the Co-Ti binary to Co-5Al-8.5W-8Ti at.%. The enhanced stability of the $L1_2$ phase predicted by Kobayashi *et al.* is apparent due to the absence of additional phases after creep at 900°C.

The differences in the cross-sectional shape changes may be attributed to differing active slip systems. Cross-sectional shape changes can indicate the active slip system(s) present during deformation [34]. The Ternary and 6Ti alloys experienced limited primary creep and the cross-sectional area in the gage sections elongated along the transverse [100] direction. This indicates that an active $\langle 1\bar{1}0\rangle\{111\}$-type slip system is present. However, the CrTa alloy experienced cross-sectional elongation along the [110] direction. This suggests that an active $\langle \bar{1}\bar{1}2\rangle\{111\}$-type system was present during deformation. Transmission electron microscopy studies are underway to investigate dislocation structure during deformation.

The creep rupture strains of the Co-base alloys are less than the Co-Ni-Al-W-base alloys studied in reference [28]. The Co-Ni-Al-W-base alloys were cast *via* the liquid metal cooling (LMC) process, which resulted in a more refined dendritic microstructure compared to the Co-base alloys presented here, so creep damage accumulation may occur at a different rate. Studies comparing the creep rupture lives of Ni-base superalloys cast *via* the LMC and Bridgman process generally show that the minimum creep rate is unaffected, but the rupture life and rupture creep strain can be affected [35].

The W-rich phases present in the ruptured specimens are similar in morphology to those observed in previous oxidation studies of the CrTa alloy and other Co-base alloys [9, 36]. Tungsten-rich phases will precipitate as the Co_3W phase if the local Al content is too low as suggested by calculated phase diagrams [8, 19, 33, 37]. A limited amount of Al loss from the sample surfaces during vacuum creep testing is likely reasonable for the formation of this phase in shear-surface regions. Assuming the shear bands arise from slip on {111} planes, nucleation of the Co_3W phase may be favorable due to the crystallographic orientation relationship between the FCC/$L1_2$ and $D0_{19}$ phases - that is $\langle 110\rangle\{111\}$ is parallel to $\langle 11\bar{2}0\rangle\{0001\}$. Rupture strains in the tested samples were in the range of 7-12% for the Ternary, 2Ta, and CrTa alloys, so these phases may have also caused a debit in creep ductiliity. Alloying strategies and/or coatings that prevent their precipitation can be developed.

Conclusions

1. Minimum creep rates at 900°C in the Co-base alloys investigated are comparable to 1st-generation Ni-base single crystal superalloy René N4.

2. Alloys which possess larger, high volume fractions of γ' precipitates exhibit lower minimum creep rates than the alloy with smaller, lower volume fractions of γ' precipitates.

3. Directional coarsening occurs during creep and rafts form parallel to the applied tensile stress, indicating positive misfit between the γ and γ' phases.

4. W-rich phases precipitate during creep at 900°C in Co-Al-W alloys with 2Ta and 1.5Ta-4.5Cr (at.%).

5. At 900°C, the Co-base alloys investigated exhibit lower minimum creep rates compared to Co-Ni-Al-W-base alloys with significant additions of Ni.

The authors acknowledge the support of the National Science Foundation (Grant DMR 1008659) and GE Energy.

References

[1] C. Sims and W. Hagel, *The Superalloys*. New York: Wiley, 1972.

[2] W. Betteridge and S. Shaw, "Development of superalloys," *Materials science and technology*, vol. 3, no. 9, pp. 682–694, 1987.

[3] *The Jet Engine*. Rolls-Royce plc, Derby, U.K.: The Technical Publications Department, 4th ed., 1992.

[4] M. Valenti, "Reaching for 60 percent," *Mechanical Engineering*, vol. 124, pp. 35–30, Apr. 2002.

[5] R. Reed, *The Superalloys: fundamentals and applications*. New York: Cambridge University Press, 2006.

[6] D. R. Clarke and C. G. Levi, "Materials design for the next generation thermal barrier coatings," *Annual Review of Materials Research*, vol. 33, no. 1, pp. 383–417, 2003.

[7] A. Suzuki, M. F. X. Gigliotti, B. T. Hazel, D. G. Konitzer, and T. M. Pollock, "Crack progression during Sustained-Peak Low-Cycle fatigue in Single-Crystal Ni-Base superalloy René N5," *Metallurgical and Materials Transactions A*, vol. 41, no. 4, pp. 947–956, 2010.

[8] J. Sato, T. Omori, K. Oikawa, I. Ohnuma, R. Kainuma, and K. Ishida, "Cobalt-Base High-Temperature alloys," *Science*, vol. 312, pp. 90–91, 2006.

[9] T. M. Pollock, J. Dibbern, M. Tsunekane, J. Zhu, and A. Suzuki, "New Co-based γ-γ high-temperature alloys," *Journal of the Minerals, Metals and Materials Society*, vol. 62, no. 1, pp. 58–63, 2010.

[10] A. Suzuki and T. M. Pollock, "High-temperature strength and deformation of γ/γ' two-phase Co-Al-W-base alloys," *Acta Materialia*, vol. 56, pp. 1288–1297, 2008.

[11] M. Tsunekane, A. Suzuki, and T. Pollock, "Single-crystal solidification of new Co-Al-W-base alloys," *Intermetallics*, pp. 636–643, 2011.

[12] A. Suzuki, G. C. DeNolf, and T. M. Pollock, "Flow stress anomalies in γ/γ' two-phase Co-Al-W-base alloys," *Scripta Materialia*, vol. 56, no. 5, pp. 385–388, 2007.

[13] M. Donachie and S. Donachie, *Superalloys: a technical guide*. Materials Park, OH: ASM Intl, 2002.

[14] S. Tin, T. M. Pollock, and W. Murphy, "Stabilization of thermosolutal convective instabilities in Ni-based single-crystal superalloys: Carbon additions and freckle formation," *Metallurgical and Materials Transactions A*, vol. 32, no. 7, pp. 1743–1753, 2001.

[15] Q. Feng, T. K. Nandy, S. Tin, and T. M. Pollock, "Solidification of high-refractory ruthenium-containing superalloys," *Acta Materialia*, vol. 51, no. 1, pp. 269–284, 2003.

[16] C. Walter, B. Hallstedt, and N. Warnken, "Simulation of the solidification of CMSX-4," *Materials Science and Engineering: A*, vol. 397, pp. 385–390, 2005.

[17] T. M. Pollock and R. D. Field, "Dislocations and High-Temperature plastic deformation of superalloy single crystals," in *Dislocation in Solids*, ch. 63, 2002.

[18] T. M. Pollock and A. S. Argon, "Directional coarsening in nickel-base single crystals with high volume fractions of coherent precipitates," *Acta metallurgica et materialia*, vol. 42, no. 6, pp. 1859–1874, 1994.

[19] S. Kobayashi, Y. Tsukamoto, T. Takasugi, H. Chinen, T. Omori, K. Ishida, and S. Zaefferer, "Determination of phase equilibria in the Co-rich Co-Al-W ternary system with a diffusion couple technique," *Intermetallics*, vol. 17, pp. 1085–1089, 2009.

[20] K. Harris, G. L. Erickson, and R. E. Schwer, "CMSX Single Crystal, CM DS and integral wheels, properties and performance," in *High Temperature Alloys for Gas Turbines and Other Applications 1986* (W. Betz, et al, ed.), (Dordrecht, Holland), pp. 719–720, D Reidel Publishing Company, 1986.

[21] J. R. Davis, *Heat-Resistant Materials*. Materials Park, OH: ASM International, 1997.

[22] P. Caron, "High *gamma*' solvus new generation nickel-based superalloys for single crystal turbine blade applications," in *Superalloys 2000*, (Seven Springs, PA), pp. 737–746, TMS, 2000.

[23] G. E. Fuchs, "Improvement of creep strength of a third generation, single crystal ni-base superalloys by solution heat treatment," *J. of Mat. Eng. Perf.*, vol. 11, no. 1, pp. 19–25, 2002.

[24] B. C. Wilson, E. R. Cutler, and G. E. Fuchs, "Effect of solidification parameters on the microstructures and properties of cmsx-10," *Mat. Sci. Eng. A*, vol. 479, no. 1, pp. 356–364, 2008.

[25] M. Ooshima, K. Tanaka, N. L. Okamoto, K. Kishida, and H. Inui, "Effects of quaternary alloying elements on the γ' solvus temperature of Co-Al-W based alloys with fcc/$L1_2$ two-phase microstructures," *Journal of Alloys and Compounds*, vol. 508, pp. 71–78, 2010.

[26] R. Schmidt and M. Feller-Kniepmeier, "Equilibrium composition and volume fraction of the γ'-phase in a Nickel-base superalloy as a function of temperature," *Scripta Metallurgica et Materialia*, vol. 26, pp. 1919–1924, 1992.

[27] D. C. Cox, B. Roebuck, C. M. F. Rae, and R. C. Reed, "Recrystallisation of single crystal superalloy CMSX-4," *Materials Science and Technology*, vol. 19, no. 4, pp. 440–446, 2003.

[28] M. S. Titus, A. Suzuki, and T. M. Pollock, "Creep and directional coarsening in single crystals of new γ-γ cobalt-base alloys," *Scripta Materialia*, vol. 66, no. 8, pp. 574–577, 2012.

[29] A. Bauer, S. Neumeier, F. Pyczak, and M. Göken, "Microstructure and creep strength of different γ/γ'-strengthened co-base superalloy variants," *Scripta Materialia*, vol. 63, no. 12, pp. 1197–1200, 2010.

[30] P. Caron and T. Khan, "Improvement of creep strength in a nickel-base single-crystal superalloy by heat treatment," *Materials Science and Engineering*, vol. 61, no. 2, pp. 173–184, 1983.

[31] H. Mughrabi, "Microstructural aspects of high temperature deformation of monocrystalline nickel base superalloys: some open problems," *Materials Science and Technology*, vol. 25, no. 2, pp. 191–204, 2009.

[32] A. Mottura, A. Janotti, and T. M. Pollock, "Alloying effects in the γ' phase of Co-based superalloys," in *Superalloys 2012*, (Seven Springs, PA), The Minerals, Metals and Materials Society, 2012.

[33] S. Kobayashi, Y. Tsukamoto, and T. Takasugi, "Phase equilibria in the Co-rich Co-Al-W-Ti quaternary system," *Intermetallics*, vol. 19, no. 12, pp. 1908–1912, 2011.

[34] N. Matan, D. C. Cox, P. Carter, M. A. Rist, C. M. F. Rae, and R. C. Reed, "Creep of CMSX-4 superalloy single crystals: effects of misorientation and temperature," *Acta Materialia*, vol. 47, no. 5, pp. 1549–1563, 1999.

[35] C. L. Brundidge, *Development of a Processing-Structure-Fatigue Model for Single Crystal Superalloys*. PhD thesis, University of Michigan, Ann Arbor, MI, 2011.

[36] L. Klein, A. Bauer, S. Neumeier, and S. Virtanen, "High temperature oxidation of γ/γ'-strengthened co-base superalloys," *Corrosion Science*, pp. 2027–2034, 2011.

[37] Y. Tsukamoto, S. Kobayashi, and T. Takasugi, "The stability of γ'-Co_3(Al,W) phase in Co-Al-W ternary system," *Materials Science Forum*, vol. 654-656, pp. 448–451, 2010.